Eng. Sci., 2025, **37**, 1795

Engineered Science

DOI: https://dx.doi.org/10.30919/es1795

New Flocculants Based on Technical Vegetable Oil – A Residue of Sunflower Oil Production

K. Zh. Abdiyev,[1] B. B. Sadykov,[1] Chien-Hsiang Chang,[2] M. B. Zhursumbayeva,[1] N. Zh. Seitkaliyeva,[1,*] G. K. Kussainova,[1] Z. N. Kambarova[1] and Zh. Toktarbay[3,4,*]

Abstract

A mixture of fatty carboxylic acids (FCA) was derived from technical vegetable oil - a residue of sunflower oil production. Chromatographic-mass spectrometric analysis revealed that the mixture primarily consists of nine types of fatty carboxylic acids. Nonionic surfactants (NIS), specifically FCA-PEG esters, were synthesized via esterification of the FCA mixture with polyethylene glycol (PEG) of molecular weights 300, 600, and 1000. The reaction yield was 93–94%. The functional composition of the resulting NIS was determined using IR and NMR spectroscopy. The critical micelle concentration (CMC), surface activity (ability to reduce the surface tension of water), maximum adsorption at the water/air interface, and other parameters of the obtained NIS particles were determined by measuring the surface tension of aqueous solutions. Among the synthesized NIS, FCA-PEG-600 exhibited the highest surface activity (Π_{CMC} = 28.8 mN/m) and maximal adsorption (Γ_{max} = 3.0×10^{-6} mol/m^2) compared to FCA-PEG-300 and FCA-PEG-1000. This "anomalous" variation in surface activity across the synthesized NIS series can be attributed to the optimal composition (i.e., the optimal hydrophilic-lipophilic balance, HLB) of the FCA-PEG-600 macromolecules. It was found that the obtained FCA-PEG NIS possess flocculating properties. Among them, the macromolecules of FCA-PEG-600 NIS demonstrated the best flocculating ability for bentonite clay suspension particles. Its optimal dosage for flocculation of suspension particles is 0.2 mg/g (200 g/t of dry solids).

Keywords: Surfactant; Adsorption; Renewable raw material; Flocculation; Water treatment.

Received: 29 August 2025; Revised: 03 October 2025; Accepted: 12 October 2025

Article Type: Original research.

1. Introduction

Surfactants are widely used in detergents, cosmetics, the textile, petrochemical, pharmaceutical, and food industries. More than half of known surfactants are synthesized from petrochemical raw materials, due to their high availability and well-established production technologies. However, the chemical processing of hydrocarbon feedstocks generates substantial carbon dioxide emissions, which contribute to the greenhouse effect in the atmosphere. Consequently, increasing global concern over fossil resource depletion, the enhanced greenhouse effect, and rising environmental pollution is driving researchers to explore renewable raw material sources.[1-4] Renewable plant-derived feedstocks represent a sustainable and environmentally friendly alternative to petrochemical products in the production of surfactants. The manufacture and application of surfactants derived from renewable plant-based raw materials do not contribute to carbon dioxide emissions, a key greenhouse gas. Plant oils,[5-7] polysaccharides, and polyglycosides[8-10] have been identified as promising feedstocks for this purpose.

Surfactants derived from alkyl polyglucosides and fatty alcohol ethoxylates are widely recognized[11-13] for their effectiveness as wetting, foaming, and cleaning agents, as well as for their synergistic performance in combination with anionic surfactants.

A wide range of nonionic and ionic surfactants based on FCA has been synthesized,[14,15] which are widely used as foaming agents,[16] emulsifiers and wetting agents.[17,18]

There is a broad spectrum of surfactants derived by modifying FCA with polyethylene oxide (PEO), which are used as nanocarriers for drug delivery.[19-23] Moreover, FCA-based surfactants have found widespread use in mineral beneficiation.[24,25]

To determine the effect of the hydroxyl group present in the hydrocarbon radical of the surfactant on micelle formation in solutions, the authors of[26] synthesized two types of nonionic surfactants using an esterification reaction: 1) from a

---

[1] *Department of Chemical Processes and Industrial Ecology, Satbayev University, Almaty 050013, Kazakhstan*

[2] *Department of Chemical Engineering, National Cheng Kung University, Tainan 70101, Taiwan*

[3] *Khoja Akhmet Yassawi International Kazakh-Turkish University, Turkestan, 161200, Kazakhstan*

mixture of stearic acid (SA) and short-chain polyethyleneglycol (PEG) and 2) from a mixture of 12-hydroxy stearic acid (HSA) and PEG. The 12-hydroxy group in HSA was previously protected to prevent interaction with PEG. It was found that in aqueous solutions, SA-PEG-SA surfactants self-assembled into 'star micelles,' whereas HSA-PEG-HSA surfactants formed 'flower micelles'.

In this case, at high concentrations in HSA-PEG-HSA surfactant solutions, flower micelles began to interact with each other by forming bridge-like hydrogen bonds between OH groups at the C_{12} alkyl chain. Intermicellar hydrogen bonds increased the stability of the hydrophobic core of micelles, consequently, the phase separation threshold was higher for HSA-PEG-HSA surfactants than for SA-PEG-SA.

The effect of ethylene oxide (EO) and propylene oxide (PO) units on the critical micelle concentration (CMC) and adsorption parameters of alkyl sulfate (C_{12}-Sulfate) has been studied in detail in.[27-30] EO units are known to increase the hydrophilicity of the molecule, thereby improving surfactant solubility in water, whereas PO units enhance lipophilicity without adversely affecting aqueous solubility. It has been established that the addition of two EO units to the structure of C_{12}-Sulfate reduces the CMC from 8.20 (for C_{12}-Sulfate) to 0.349 mmol/L (for C_{12}-$(EO)_2$-Sulfate) and decreases the surface tension of the surfactant solution at CMC (σ_{CMC}) from 39.5 to 26.5 mN/m.[27,28,30] The incorporation of a PO group into C_{12}-Sulfate was found to have little effect on the σ_{CMC} value, while significantly decreasing the CMC. At the same time, the degree of reduction depends on the number of incorporated PO units (from 0.420 mmol/L for C_{12}-$(PO)_4$-Sulfate to 0.043 mmol/L for C_{12}-$(PO)_{12}$-Sulfate).[29,30]

It has been shown that the incorporation of EO units into C_{12}-Sulfate does not lead to a significant change in the value of the maximum adsorption (Γ_{max}).[27,28] In contrast, when PO units are introduced into the alkyl sulfate structure, a decrease in Γ_{max} is observed from 3.16×10^{-10} mol/cm^2 (for C_{12}-Sulfate) to 1.01×10^{-10} mol/cm^2 (for C_{12}-$(PO)_{4\text{-}12}$-Sulfate). The incorporation of PO units into alkyl sulfate significantly increases the area occupied by the surfactant molecule in the saturated adsorption layer. The maximum increase (from 0.53 nm^2 for C_{12}-Sulfate to 1.66 nm^2 for C_{12}-$(PO)_4$-Sulfate) already occurs with the incorporation of only 4 PO units.[29,30]

The addition of EO and PO units also increases pC_{20} (pC_{20} = -log (C_{20}) and the CMC/C_{20} ratio (where C_{20} is the concentration of the surfactant solution at which the surface tension of water decreases by 20 mN/m) several fold.[28-30] With an increase in PO content from 4 to 12 units in C_{12}-$(PO)_x$-Sulfate, the CMC/C_{20} parameter increases from 11.6 to 42.2. These data indicate that the incorporation of EO and PO into alkyl sulfate significantly enhances the adsorption activity of alkyl sulfate.

According to,[31] the CMC and A_{min} parameters of the C_{12}-$(PO)_y$/$(EO)_z$-Head surfactants (where Head is the polar functional group) depend not only on the number and sequence (sequential and homogeneous) of PO and EO units attached to the main chain, but also on the nature, structure, and charge (degree of dissociation) of the polar head functional group. It has been established that the attachment of a bulky polar group (carboxylate, sulfate, and disodium phosphate) to the main chain of the surfactant leads to a significant increase in CMC (from 0.011 to 0.019–0.20 mmol/L) and A_{min} (from 0.65 to 1.70–7.20 nm^2) for the given surfactant. At the same time, surfactants with homogeneously attached EO and PO units occupy a larger area (A_{min}) and have relatively high CMC values compared to surfactants with a sequential structure.

The literature review highlights a lack of research on the use of waste sunflower oil for surfactant synthesis and property evaluation. The present study therefore aims to develop eco-friendly nonionic surfactants (flocculants) from sunflower-oil by-products and polyethylene glycol and to assess their physicochemical and surface-active properties.

2. Experimental

2.1 Materials

Technical vegetable oil – a residue of sunflower oil production – was used as the hydrophobic fragment for the synthesis of NIS. A mixture of FCA was isolated from the technical vegetable oil using methods of alkaline hydrolysis, acid treatment, and extraction. The procedure for isolating the FCA mixture is described in detail in.[32]

Concentrated solutions of sodium hydroxide and sulfuric acid (purity ≥ 95 wt %) were employed for the hydrolysis of fatty acid esters.

Polyethylene glycol (PEG) with molecular weights of 300, 600, and 1000 (produced by Sigma Aldrich, compound purity ≥ 98 wt. %) was used as the hydrophilic fragment for the synthesis of NIS.

The flocculating properties of the synthesized surfactants were studied in a suspension of bentonite clay from the Tagan deposit (Eastern Kazakhstan). The rheological and technological characteristics of the bentonite clay are as follows: density – 1.04 g/cm^3, sand content – 1.0%, moisture content of the clay powder – 14%, suspension pH – 7, conditional viscosity – 25 seconds, yield of clay solution – 16–20 m^3/t, and thixotropy index – 2 mgs/(cm×min).

2.2 Methods

The IR spectrum of the fatty carboxylic acid mixture was observed using a Nicolet 5700 FTIR spectrometer (Thermo Corporation, USA) in the frequency range of 4000–500 cm^{-1}. ^{1}H and ^{13}C NMR spectra were obtained on a JNM-ECA Jeol 400 NMR spectrometer operating at 399.78 MHz and 100.53 MHz, respectively, using $CDCl_3$ as the solvent. Chemical

---

[4] Institute of Sustainability of Ecology and Bioresources, Al-Farabi Kazakh National University, Almaty, 050040, Kazakhstan

[*] E-mail: n.seitkaliyeva@satbayev.university (N. Zh. Seitkaliyeva), zhexenbek.toktarbay@gmail.com (Zh. Toktarbay)

shifts were referenced to the residual proton and carbon signals of deuterated chloroform.

Gas chromatography–mass spectrometry (GC–MS) analysis of the mixture was performed using an Agilent 7890B gas chromatograph equipped with an Agilent 5977B quadrupole mass-selective detector (ionization energy: 70 eV; ion source temperature: 230 °C; quadrupole temperature: 150 °C), following the procedure described in.[33,34] Separation was carried out on a HP-5ms UI capillary column (30 m × 0.25 mm i.d., 0.25 μm film thickness; Agilent, USA). Helium was used as the carrier gas at a flow rate of 1 mL/min. Sample introduction was performed in split mode (1:20). The oven temperature program was as follows: isothermal at 80 °C for 2 minutes, then ramped to 280 °C at a rate of 5 °C/min. The injector temperature was set at 280 °C; injection volume was 1 μL. The detector interface temperature was maintained at 280 °C. The mass scan range was 30–550 m/z.

The software used for processing the chromatographic–mass spectrometric data included MassHunter Qualitative Analysis (Version B.06.00, Agilent Technologies), NIST MS Search 2.0, and the NIST11 mass spectral library (release date: May 19, 2011).[33]

The surface tension (σ) of aqueous surfactant solutions at the water/air interface was measured at room temperature using the Wilhelmy plate method with a SZFL-A1 tensiometer (model A1 series).[35] The measurement accuracy was 0.1 mN/m. In this method, a platinum plate is gradually lowered into a surfactant solution until it comes into contact with the surface. After contact, the force required to detach the plate from the surface is measured. Based on the measured detachment force, surface tension is calculated using the following Eq. (1):

$$\sigma = F / (L \times \cos \theta) \qquad (1)$$

where σ is the surface tension of the solution (mN/m), F is the detachment force (mN), L is the perimeter of the wetted part of the plate ($L = 2 \cdot l$, where l is the width of the lower edge of the plate), in meters.

Due to the roughness of the platinum plate surface, complete wetting occurs ($\theta = 0$), and therefore $\cos \theta = 1$. Surface tension for each solution was measured five times, and the arithmetic mean value of σ was reported.

To evaluate the surface activity of the synthesized surfactants, the following parameters were determined:

1. Surface pressure Eq. (2) at the critical micelle concentration (π_{CMC}) was calculated as the difference between the surface tension of water (σ_0) and that of the surfactant solution at the CMC (σ_{CMC}):[36,37]

$$\Pi_{CMC} = \sigma_0 - \sigma_{CMC} \qquad (2)$$

2. Maximum surface excess concentration (Γ_{max}) at the water/air interface was determined from the surface tension isotherm $\sigma = f(\ln C)$, using the Gibbs adsorption Eq. (3):[38-40]

$$\Gamma_{max} = - a / R \times T \times n \qquad (3)$$

where a is the slope of the linear portion of the σ vs. ln C plot below the CMC (*i.e.*, $a = (d\sigma/\ln C)$, R is the universal gas constant (8.314 J/(mol×K)), T is the absolute temperature (K) and n is the number of species adsorbed at the interface. For nonionic surfactants, $n = 1$.

3. Minimum area per molecule (A_{min}) in the saturated adsorption layer was calculated according Eq. (4):[39,40]

$$A_{min} = 10^{18} / N_A \times \Gamma_{max} \qquad (4)$$

where N_a is Avogadro's number (6.022×10^{23} mol^{-1}).

4. pC_{20}, an empirical parameter characterizing the efficiency of surface tension reduction, was calculated using the following Eq. (5):[41]

$$pC_{20} = - \log (C_{20}) \qquad (5)$$

where C_{20} is the surfactant concentration at which the surface tension of water is reduced by 20 mN/m.

The acid number of the oil (X, mg KOH/g) was calculated using the following Eq. (6):[42]

$$X = (5.611 \times V) / m \qquad (6)$$

where 5.611 is the mass of KOH in 1 cm^3 of a solution with a molar concentration of c(KOH)=0.1 mol/dm^3, mg, V is the volume of a KOH solution with a molar concentration of c(KOH) = 0.1 mol/dm^3, spent on titration, cm^3 and m is the mass of the sample, g.

The elemental composition of bentonite clay was determined using energy-dispersive X-ray fluorescence spectroscopy (EDXRF, USA, 2024). The analysis was carried out using a Rigaku NEX CG II X-ray fluorescence spectrometer. This instrument utilized four secondary targets: aluminum (Al), molybdenum (Mo), copper (Cu), and RX9. The tube voltages were 50, 50, 50, and 25 kV, respectively, while the currents were set to 1, 1, 1, and 2 mA. The exposure time for each target was set within the range of 100–200 seconds. The samples were preliminarily ground using a FULVERISETTE 2 automatic mortar grinder made of stainless steel. For analysis, the samples were placed under a 4 μm polypropylene film and analysed in powder form.

At the initial stage of the experiment, the bentonite clay was ground in a mill at a speed of 300 rpm for 10 minutes, and the resulting powder was then passed through a sieve with a mesh size of 0.1 mm. After that, 0.3 g of the powder was placed in a graduated cylinder, 99.7 mL of distilled water was added (0.3 wt. %), and the suspension was left in a closed container for 24 hours to allow swelling. Before use, the suspension was mixed in a mixer for 3 minutes at a speed of 100 rpm. Then, 10 mL of the suspension was transferred into several test tubes, and the required amounts of surfactant solution were added under vigorous stirring.

Flocculation of bentonite particles in the presence and absence of surfactants was studied by measuring the optical density (OD) of the suspension. OD was measured using an i3

UV-VIS spectrometer (China) at a wavelength of incident light of 546 nm. Bidistilled water was used as the standard. The residual turbidity (RT, %) was calculated according to the following Eq. (7):[43,44]

$$RT = (OD_{546s} / OD_{546i}) \times 100\% \qquad (7)$$

where OD_{546s} denotes OD_{546} after the addition of the flocculant and OD_{546i} denotes OD_{546} of the suspension in the absence of flocculant under the same experimental conditions.

The electrokinetic (zeta) potential (ζ) of surfactant colloidal particles in aqueous solutions at the CMC concentration, as well as that of the bentonite suspension, was determined at room temperature using a Zetasizer Advance Series ZSU3200-Pro (Blue Label) manufactured by Malvern Panalytical. The value of the zeta potential was calculated using software based on the Helmholtz–Smoluchowski equation. The measurement error did not exceed 1%. The average value was calculated based on three measurements.

All surfactant solutions and suspensions were prepared using bidistilled water.

3. Results and discussion

3.1 Analysis of the chromatography–mass spectrometry results of the extract obtained from the hydrolysis product of technical vegetable oil

To determine the composition of the mixture obtained after the hydrolysis of technical vegetable oil and the extraction of fatty carboxylic acids, a chromatography–mass spectrometry analysis of the mixture was performed. For this purpose, the fatty carboxylic acids in the mixture were preliminarily converted into methyl esters by means of an esterification reaction. The results of the chromatography–mass spectrometry analysis are presented in Fig. 1 and Tables 1 and 2.

According to the fragmentation mechanism of fatty carboxylic acids resulting from electron ionization (EI) of the

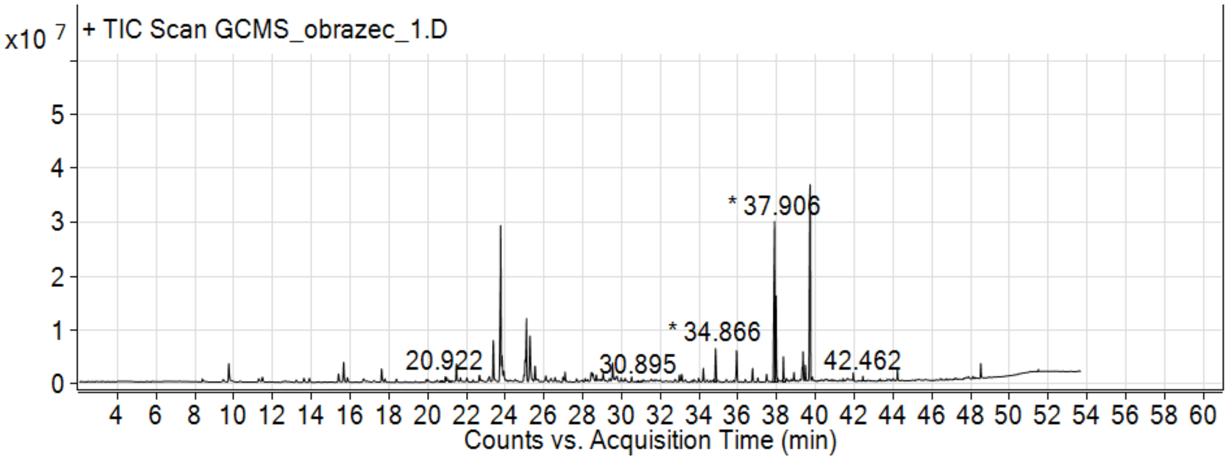

Fig. 1: Chromatogram of the extract (methyl esters of fatty carboxylic acids) obtained from the hydrolysis product of technical vegetable oil.

Table 1: User chromatogram peak list.

RT	Height	Height %	Area	Area %	Area Sum %	Sym-metry	Width
20.741	277218.32	0.93	2447951.6	2.49	1.34	1	0.25
20.922	1000995.5	3.35	3100876.84	3.16	1.7	0.63	0.095
21.12	348225.12	1.16	1918437.48	1.95	1.05	2.33	0.146
30.895	318313.78	1.06	2614859.57	2.66	1.43	0.6	0.258
34.866	6338783.5	21.18	20394066.08	20.75	11.18	1.4	0,129
37.906	29921448.68	100	98282399.33	100	53.88	0.46	0.129
37.992	16050644.47	53.64	37760134.75	38.42	20.7	0.77	0.103
38.363	4725054.69	15.79	13149403.69	13.38	7.21	3.02	0.155
42.462	978826.63	3.27	2741811.75	2.79	1.5	3.6	0.189

Table 2: Content of methyl esters of fatty carboxylic acids.

Compound Label	RT	Name	Area Sum, %
Cpd 1: 2-Decenoic acid, methyl ester	20.741	2-Decenoic acid, methyl ester	1.34
Cpd 2: 4-Decenoic acid, methyl ester	20.922	4-Decenoic acid, methyl ester	1.7
Cpd 3: Decanoic acid, methyl ester	21.12	Decanoic acid, methyl ester	1.05

Compound Label	RT	Name	Area Sum, %
Cpd 4: Oxiraneundeca-noic acid, 3-pentyl-, methyl ester, cis-	30.895	Oxiraneundecanoic acid, 3-pentyl-, methyl ester, cis-	1.43
Cpd 5: Hexadecanoic acid, methyl ester	34.866	Hexadecanoic acid, methyl ester	11.18
Cpd 6: 9,12-Octadeca-dienoic acid (Z,Z)-, methyl ester	37.906	9,12-Octa-decadie-noic acid (Z,Z)-, methyl ester	53.88
Cpd 7: 9-Octadecenoic acid (Z)-, methyl ester	37.992	9-Octadecenoic acid (Z)-, methyl ester	20.7
Cpd 8: Methyl stearate	38.363	Methyl stearate	7.21
Cpd 9: Docosanoic acid, methyl ester	42.462	Docosanoic acid, methyl ester	1.5

analyzed compounds, base peaks characteristic of the studied fatty acids were identified.[33,34] The identification of components in the reaction mixture, represented as peaks on the chromatogram, was carried out based on the analysis of the mass spectra of each compound. Through detailed examination of the mass spectra and according to the fragmentation mechanism under electron ionization, the composition of the methyl esters of fatty carboxylic acids (FCA) was determined and presented in Table 2. The results of the chromatography–mass spectrometry analysis are expressed as the percentage content of individual methyl esters of fatty acids. The analysis was performed using a flame ionization detector (FID), which allows the peak areas to be interpreted as relative mass fractions.

As shown in Table 2, the mixture of fatty carboxylic acids consists of 9 types of saturated and unsaturated acids, with the highest mass fractions corresponding to 9,12-octadecadienoic acid (linoleic acid) and 9-octadecenoic acid (oleic acid). In addition to fatty carboxylic acids, other cycloaliphatic and unsaturated cyclic organic compounds were also detected, including: 2,6,6-trimethylbicyclo[3.1.1]hept-2-ene, bicyclo[3.1.0]hexane, 4-methylene-1-(1-methylethyl)-, and 2-(1R,4R)-4-hydroxy-4-methylcyclohex-2-enyl)propan-2-yl acetate.

3.2 Synthesis of nonionic surfactants

For the synthesis of nonionic surfactants from a mixture of fatty carboxylic acids, polyglycols were selected as hydrophilic reagents: polyethylene glycol-300 (PEG-300), polyethylene glycol-600 (PEG-600), and polyethylene glycol-1000 (PEG-1000). The main reason for choosing PEG was the ability to vary the molar amount of ethylene oxide (hydrophilic) fragments in the structure of the resulting ester (R–CO–[O–C_2H_4]$_n$–OH). By adjusting the number of ethylene oxide groups, the hydrophility (hydrophilic-lipophilic balance, HLB) of the resulting NIS can be altered. As a rule, as the number of ethylene oxide fragments in the NIS increases, its water solubility improves and the HLB value increases. Therefore, by modifying the ethylene oxide content in the NIS, it is possible to synthesize surfactants tailored for various purposes (flocculant, detergent, emulsifier, flotation reagent, wetting agent, foaming agent, etc.).

Synthesis of a nonionic surfactant from a mixture of fatty carboxylic acids (FCA) and polyethylene glycol-300 (PEG-300)

The reaction was carried out in a three-neck flask equipped with a magnetic stirrer, a thermometer, and a Dean–Stark apparatus for removing water from the reaction medium. Into the flask, 0.45 mol of PEG-300 and a catalyst (p-toluenesulfonic acid, 1% of the total mass) were introduced. After mixing the catalyst with PEG-300, the required amount of the FCA mixture was added. The molar ratio of the reagents FCA:PEG-300 in the reaction medium was 1:1.2. The condensation reaction was performed in a flask heater at a temperature of 140–150°C for 3 hours under continuous stirring in an argon atmosphere. As a result of the reaction, an ester of fatty acids with PEG-300 was formed Eq. (8):

$$\text{R-COOH} + \text{HO-[CH}_2\text{-CH}_2\text{-O-]}_n\text{H} = \text{R-COO-[CH}_2\text{-CH}_2\text{-O-]}_n\text{H} + \text{H}_2\text{O} \qquad (8)$$

The reaction was carried out until the acid number of the mixture reached a constant value. The amount of ester formed during the reaction (reaction yield) was calculated based on the volume of water collected in the Dean–Stark apparatus and from the acid number of the mixture (Fig. 2).[42]

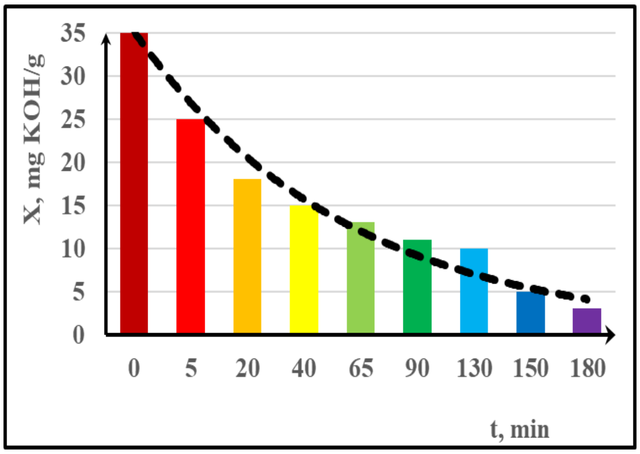

Fig. 2: Change in the acid number of the mixture during the synthesis of NIS from a mixture of FCA and PEG-300.

At the end of the reaction, the reaction mass was dried in a vacuum drying oven at 50 °C. The reaction yield, calculated based on the acid number, was 94%. The product is a viscous brown liquid.

Synthesis of a nonionic surfactant from a mixture of fatty carboxylic acids (FCA) and polyethylene glycol-600 (PEG-600)

The esterification reaction of fatty carboxylic acids with PEG-600 was carried out under the same conditions as in the case of PEG-300. The reaction temperature was 150–160 °C. The reaction yield, calculated based on the acid number (Fig. 3), was 94%.[42] The product is a viscous brown liquid.

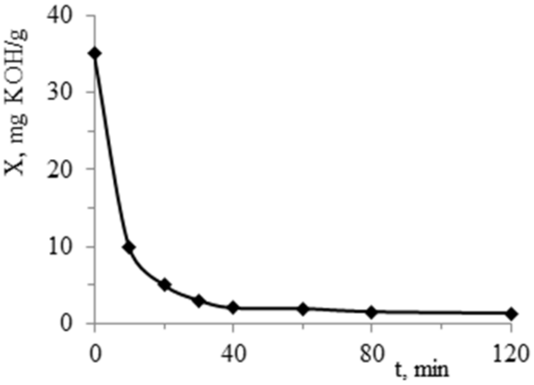

Fig. 3: Change in the acid number of the mixture during the synthesis of NIS from a mixture of FCA and PEG-600.

Synthesis of a nonionic surfactant from a mixture of fatty carboxylic acids (FCA) and polyethylene glycol-1000 (PEG-1000)

The esterification reaction of fatty carboxylic acids with PEG-1000 was carried out under the same conditions as in the case of PEG-300. The reaction temperature was 160–170 °C. The reaction yield, calculated based on the acid number (Fig. 4), was 93%.[42] The product is a viscous brown liquid.

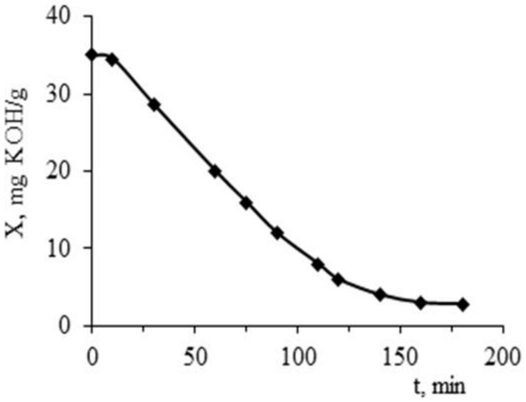

Fig. 4: Change in the acid number of the mixture during the synthesis of NIS from a mixture of FCA and PEG-1000.

3.3. Analysis of the IR and NMR spectrum of the obtained nonionic surfactants

IR Spectra of the NIS Synthesized from a Mixture of FCA and Polyethylene Glycol-300 (PEG-300)

In the IR spectrum (Fig. S1, please see supporting information), a band at 1736 cm^{-1} is observed, corresponding to the carbonyl group of saturated carboxylic acids, while the band at 1644 cm^{-1} is characteristic of the carbonyl group in unsaturated carboxylic acids.

The absorption band associated with the free hydroxyl group of ethylene glycol appears at 3415 cm^{-1}, and absorption bands in the range of 2860–2924 cm^{-1} correspond to hydrogen-bonded hydroxyl groups in PEG-300.[45,46] Additionally, the band at 1106 cm^{-1} corresponds to the $–CH_2–O–CH_2–$ stretching vibration in the ester bonds of carboxylic acid derivatives.

These IR spectral features confirm that a fatty acid ester is formed during the reaction between FCA and PEG-300.

NMR Analysis of the NIS Based on the FCA and PEG-300 Mixture in $CDCl_3$

NMR spectra of the obtained surfactant are presented in Fig. S2-S6. The ^{1}H NMR spectrum of the fatty acid esters synthesized from FCA and PEG-300 displays signals corresponding to protons from various fragment structures across the full spectral range (Fig. S2). In the region from 0.50 to 3.30 ppm, signals from methyl and methylene protons of fatty acid residues and PEG-300 fragments are observed. This is the most abundant group of fragments in the mixture of fatty acid esters with PEG-300, with a total integral proton intensity of 146.33H.[46]

Signals in the range of 3.30–4.50 ppm correspond to protons adjacent to oxygen atoms or other electronegative functional groups. Their integral proton intensity amounts to 30.63 H.

Proton signals from the fatty acid residues observed in the 4.50–6.40 ppm range belong to unsaturated moieties of the carboxylic acids, with an integral intensity of 45.47 H. The remaining signals in the 6.70–7.40 ppm region indicate the presence of aromatic protons in the ester mixture of FCA with PEG-300, with a proton intensity of 1.94 H.

Based on these results, it can be concluded that in the mixture of fatty acid esters with PEG-300, the fraction of protons adjacent to oxygen atoms increases, reaching 13.65 %. Moreover, the aromatic character of the esters decreases, as indicated by the drop in aromatic proton content from 2.54 % in the initial fatty acids to 0.84% in the ester mixture.

In the ^{13}C NMR spectrum of the mixture of fatty carboxylic acid (FCA) esters with polyethylene glycol-300 (PEG-300), the signals of the carbon atoms in methyl and methylene groups appear in the range of 10.00–49.32 ppm (Fig. S3). The signals of carbon atoms adjacent to oxygen atoms or other electronegative groups are shifted further downfield, appearing in the region of 49.32–73.00 ppm. The integral intensity of these carbon nuclei is 393.17.

A minor set of signals in the region of 110.00–160.00 ppm corresponds to the carbon atoms of unsaturated groups, with an integral intensity of 7.93. The presence of an ester group and carboxyl group residues in the mixture of FCA esters with PEG-300 is confirmed by a signal at 174.23 ppm in the carbon spectrum, with an integral intensity of 0.85.

The structure of the FCA-PEG-300 ester mixture was further confirmed using two-dimensional NMR spectroscopy methods: COSY (^{1}H–^{1}H), HMQC (^{1}H–^{13}C), and HMBC (^{1}H–^{13}C), which enable the identification of homo- and heteronuclear spin-spin couplings. The observed correlations in the COSY, HMQC, and HMBC spectra of the FCA-PEG-300 esters are presented in Fig. S4–S6 (please see supporting information), confirming the previously stated assumptions regarding the formation of the FCA-PEG-300 surfactant.

IR spectra of the nonionic surfactant synthesized from a mixture of FCA and polyethylene glycol-600 (PEG-600)

In the IR spectrum (Fig. S7), an absorption band at 1737 cm^{-1} corresponds to the carboxyl group of saturated fatty acids, while a band at 1644 cm^{-1} is characteristic of the carboxyl group of unsaturated fatty acids.[45,46] An absorption band typical of free hydroxyl groups of polyethylene glycol is observed at 3396 cm^{-1}. Bands in the 2871–2912 cm^{-1} range correspond to hydroxyl groups of PEG-600 involved in intermolecular hydrogen bonding.[45,46] A broad absorption band at 1107 cm^{-1} corresponds to the –CH$_2$–O–CH$_2$– bonds present in esters of carboxylic acids. Thus, based on the IR spectrum, it can be concluded that the reaction between FCA and PEG-600 leads to the formation of an ester.

Analysis of the NMR spectra of NIS based on FCA and polyethylene glycol-600 (PEG-600) in CDCl$_3$ solvent

NMR spectra of the obtained surfactant are presented in Fig. S8 – S12. The ^{1}H NMR spectrum of fatty acid esters with polyethylene glycol-600 is characterized by the presence of signals corresponding to protons from various fragmental structures across the entire spectral range (Fig. S8). In the region of 0.50–3.30 ppm, signals are observed for protons of methyl and methylene groups from the FCA and PEG-600 fragments. The integral proton intensity in this region is 99.54H[40] Signals in the range of 3.30–4.50 ppm correspond to protons adjacent to oxygen atoms or other electronegative functional groups. These signals exhibit the highest integral proton intensity, amounting to 158.59H. The proton signals of fatty acid residues observed in the region of 4.50–6.40 ppm correspond to the unsaturated fragments of carboxylic acids. Their integral proton intensity is 4.62 H. The remaining signals in the range of 6.70–7.40 ppm indicate the presence of aromatic protons in the composition of the FCA–PEG-600 esters, with an integral intensity of 0.02 H. Based on the above results, it can be concluded that in the mixture of FCA–PEG-600 esters, the proportion of protons located adjacent to oxygen atoms increases to 60.37%. This indicates a significant increase in the polyethylene glycol content in the ester products. Furthermore, due to the reaction of the fatty acid mixture with PEG-600, the aromatic contribution in the esters is reduced to zero.

The ^{13}C NMR spectrum of the mixture of fatty carboxylic acid esters with PEG-600 (Fig. S9) shows signals of carbon atoms from methyl and methylene groups in the range of 10.00–49.32 ppm. The signals of carbon atoms adjacent to oxygen atoms or other electronegative atoms appear further downfield in the range of 49.32–73.00 ppm. The integral carbon intensity of these nuclei is 317.01.

A minor group of signals observed in the range of 110.00–160.00 ppm corresponds to the carbon atoms of unsaturated moieties, with their integral intensity being close to zero. Due to the significant enrichment of the ester mixture with PEG-600 fragments, the content of ester groups has substantially decreased, and these signals do not appear in the carbon spectrum.

The structure of the mixture of FCA esters with PEG-600 was further confirmed by two-dimensional NMR spectroscopy methods: COSY (^{1}H–^{1}H), HMQC (^{1}H–^{13}C), and HMBC (^{1}H–^{13}C), which allow the identification of homo- and heteronuclear spin–spin couplings. The observed correlations in the COSY, HMQC, and HMBC spectra of the FCA–PEG-600 esters are presented in Fig. S10 – S12, confirming the above conclusions regarding the formation of the FCA–PEG-600 surfactant.

IR Spectra of the Nonionic Surfactant Synthesized from a Mixture of Fatty Carboxylic Acids (FCA) and Polyethylene Glycol-1000 (PEG-1000)

In the IR spectrum (Fig. S13), an absorption band corresponding to the carboxyl group of saturated carboxylic acids is observed at 1736 cm^{-1}, and a band characteristic of the carboxyl group of unsaturated carboxylic acids is observed at 1644 cm^{-1}.[45, 46]

The absorption band typical of free hydroxyl groups of polyethylene glycol is observed at 3412 cm^{-1}, and in the range of 2873–2917 cm^{-1}, absorption bands corresponding to the hydroxyl groups of polyethylene glycol-1000 (PEG-1000) involved in hydrogen bonding with each other are observed[45,46]. A broad band corresponding to –CH$_2$–O–CH$_2$– linkages in the esters of carboxylic acids is observed at 1109 cm^{-1}.

Thus, based on the IR spectrum, it can be concluded that a fatty acid ester is formed as a result of the reaction between fatty carboxylic acids and polyethylene glycol-1000 (PEG-1000).

Analysis of NMR Spectra of the Nonionic Surfactant Based on Fatty Carboxylic Acids (FCA) and Polyethylene Glycol-1000 (PEG-1000) in CDCl$_3$ Solvent

NMR spectra of the obtained surfactant are presented in Fig. S14 – S18.

The ^{1}H NMR spectrum of fatty acid esters with polyethylene glycol-1000 (PEG-1000) is characterized by the presence of signals from protons of various structural fragments across the entire spectral range (Fig. S14). In the range of 0.50–3.30 ppm, signals corresponding to the protons of methyl and methylene groups of the FCA and PEG-1000 fragments are observed. Their integral proton intensity is 103.38 H. The signals in the region of 3.30–4.50 ppm correspond to protons located adjacent to oxygen atoms or other electronegative functional groups. Their integral proton intensity is the highest and amounts to 94.04 H.[46]

The proton signals of fatty acid residues observed in the region of 4.50–6.40 ppm belong to the unsaturated fragments of carboxylic acids. Their integral proton intensity is 9.95 H. The remaining signals in the region of 6.70–7.40 ppm indicate the presence of aromatic protons in the composition of the FCA and PEG-1000 esters, with an integral proton intensity of 0.44 H.

Based on the above results, it can be concluded that in the mixture of FCA and PEG-1000 esters, the proportion of protons located adjacent to oxygen atoms increases and reaches 45.25%. These results indicate a substantial increase in the proportion of polyethylene glycol (PEG) fragments in the FCA esters synthesized with PEG-1000.

The combined proportion of protons from methyl and methylene groups of the FCA and PEG-1000 moieties is also high, accounting for 49.75%. In addition, the aromatic proton content decreases to 0.2% as a result of the interaction between the FCA mixture and PEG-1000.

In the ^{13}C NMR spectrum of FCA esters with PEG-1000, signals of carbon atoms from methyl and methylene groups appear in the region of 10.00–49.32 ppm (Fig. S15).[46] Signals of carbon atoms adjacent to oxygen or other electronegative atoms are observed further downfield in the range of 49.32–73.00 ppm. The total carbon integral intensity for these nuclei is 383.18. A small group of signals observed in the 110.00–160.00 ppm region corresponds to carbon atoms of unsaturated groups, with an integral intensity close to zero. Due to the high enrichment of the FCA esters with polyethylene glycol fragments, the content of ester groups is significantly reduced and they are not observed in the carbon spectrum.

The structure of the FCA esters with PEG-1000 was also confirmed by two-dimensional NMR spectroscopy methods: COSY (^1H–^1H), HMQC (^1H–^{13}C), and HMBC (^1H–^{13}C), which make it possible to identify homo- and heteronuclear spin–spin couplings. The observed COSY (^1H–^1H), HMQC (^1H–^{13}C), and HMBC (^1H–^{13}C) correlations in the FCA esters with PEG-1000 are presented in Fig. S16 – S18. These data confirm the earlier assumptions regarding the formation of the FCA-PEG-1000 surfactant.

3.4 Surface activity of surfactants based on FCA-PEG at water/air interface

To evaluate the surface activity of the surfactants, the surface tension of aqueous solutions of PEGs and the nonionic surfactants (NIS) synthesized from them was measured (Fig. 5). According to the surface tension isotherms, individual PEGs demonstrate limited ability to reduce the surface tension of water. From these isotherms, the critical micelle concentrations (CMC) and the corresponding surface tension values at the CMC (σ_{CMC}) were determined. The results of these calculations are presented in Tables 3 and 4. The data indicate that the FCA-PEG-600 surfactant exhibits the highest surface activity – *i.e.*, the greatest ability to reduce the surface tension of water–compared to FCA-PEG-300 and FCA-PEG-1000. This "anomalous" trend in surface activity among the synthesized NIS samples can be attributed to the optimal hydrophilic–lipophilic balance (HLB) of the FCA-PEG-600 macromolecules. This assumption is further supported by the zeta potential measurements: FCA-PEG-600 shows the lowest zeta potential among the tested surfactants (Table 3).

It is known that the FCA residue imparts hydrophobicity to

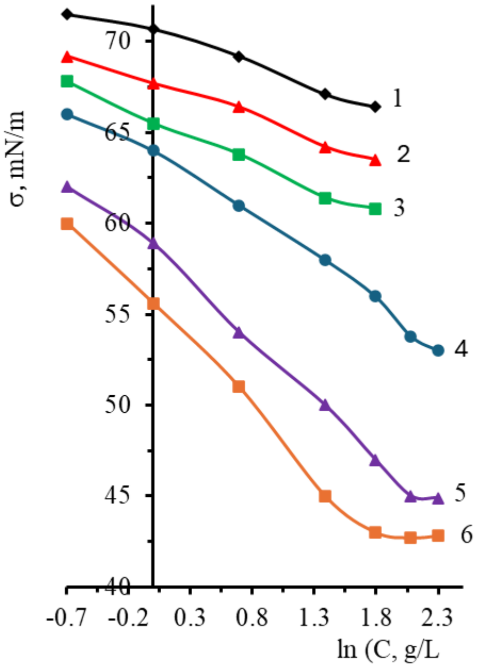

1 – PEG-300; 2 – PEG-600; 3 – PEG-1000; 4 – FCA-PEG-300 surfactant; 5 – FCA-PEG-1000 surfactant; 6 – FCA-PEG-600 surfactant.

Fig. 5: Surface tension isotherms of aqueous solutions of PEG (1–3) and FCA-PEG surfactants (4–6). T = 298 K.

Table 3: Micellization parameters and zeta-potential of surfactant colloidal particles in aqueous surfactant solutions. T = 298 K.

Surfactant	CMC, g/l	σ_{CMC}, mN/m	Π_{CMC}, mN/m	ζ_{CMC}, mV
FCA-PEG-300	10.0	53.0	18.8	-22,5
FCA-PEG-600	6.0	43.0	28.8	-5,7
FCA-PEG-1000	8.0	45.5	26.3	-10,1

Table 4: Adsorption parameters of the surfactants.

Surfactant	$\Gamma_{max}\times10^6$, mol/m^2	A_{min}, nm^2	C_{20}, g/l	pC_{20}	CMC/C_{20}
FCA-PEG-300	1.9	0.87	-	-	-
FCA-PEG-600	3.0	0.55	1.82	-0.26	3.3
FCA-PEG-1000	2.7	0.62	3.00	-0.48	2.7

the surfactant macromolecules, whereas the ethoxy groups contribute hydrophilicity. However, an excessively long hydrocarbon radical can significantly reduce the water solubility of the surfactant, resulting in the loss of the molecule's ability to adsorb at the water/air interface. In contrast, ethoxy groups in the structure of FCA-PEG surfactants enhance the water solubility of surfactant macromolecules, thereby increasing their ability to adsorb at the water/air interface. Nonetheless, the presence of excessively long ethoxy groups may lead to an increase in the hydrophilic-lipophilic balance (GLB) and a slight decrease in the surface activity of FCA-PEG surfactants. A clear example of this is the comparison of the surface tension isotherms of PEG-600 and the FCA-PEG-600 surfactant: PEG-600 macromolecules exhibit relatively low ability to reduce the surface tension of water ($\Delta\sigma \approx 8$ mN/m) compared to FCA-PEG-600 ($\Delta\sigma \approx 28$ mN/m) (Fig. 5).

Thus, based on the above, it can be concluded that the FCA-PEG-600 surfactant has an optimal GLB value, which ensures maximum surface activity of its macromolecules.

The σ_{CMC} values of the synthesized FCA-PEG-based NIS are higher than those of alkyl glucosides, fatty alcohol ethoxylates, sodium soap salts[37,47] and C_{12}-Sulfate,[27] including sodium oleate and sodium laurate.[35] But they are lower than those of sodium hexanoate (at pH 6–10).[35]

Among the synthesized surfactants, FCA-PEG-600 exhibits the highest adsorption and, consequently, the smallest surface area occupied by a single molecule in the saturated adsorption layer (A_{min}) (Table 4). These data indicate that FCA-PEG-300 molecules adopt a more compact conformation compared to other FCA-PEG surfactants. This compact conformation is stabilized by hydrophobic interactions between hydrocarbon radicals and hydrogen bonding between hydroxyl groups.

According to the A_{min} value, FCA-PEG-300 is close in properties to soap (0.93 nm^2)[37] and *n*-tert-octylphenyl ether of hexadecaethylene glycol (0.80 nm^2).[18] In contrast, the minimal surface areas of FCA-PEG-600 and FCA-PEG-1000 are similar to those of C_{12}-Sulfate (0.53 nm^2)[27] and *n*-tert-octylphenyl ether of octaethylene glycol (0.58 nm^2).[48]

The parameter Π_{CMC} demonstrates the ability of a surfactant to reduce the surface tension of water, and the CMC/C_{20} parameter indicates if the surfactant preferably adsorbs to the surface or aggregates into micelles.[37,30] A high CMC/C_{20} ratio shows a high adsorption capacity of the surfactant at the water/air interface. On the contrary, small ratio indicates a high miccellization capacity of the surfactant.[30]

The parameters of Π_{CMC} for FCA–PEG-600 and FCA-PEG-1000 are higher than those for FCA–PEG-300. But the parameters of Π_{CMC} and CMC/C_{20} for synthesized FCA–PEGs are much lower than that of alkylpolyglucoside, sodium soap and alkylethoxylated fatty alcohol (AE) (44.5-51.2 mN/m).[37] The CMC/C_{20} values of FCA-PEG-600 and FCA-PEG-1000 surfactants are close to the value of C_{12}-Sulfate (2.6).[30]

The relatively low values of *p*CMC and CMC/C_{20} (Table 4) can be attributed to the oligomeric (polymeric) nature of the obtained NIS molecules. The compact conformation of the molecules, stabilized by intramolecular hydrophobic interactions between hydrocarbon radicals and hydrogen bonds between terminal hydroxyl groups,[49,50] hinders the orientation (differentiation) of individual segments of the surfactant molecules by polarity at the water/air interface.[51,52] As a result, this ultimately leads to a reduced ability of the surfactant molecules to decrease the surface tension of water. The relatively low values of *p*CMC and CMC/C_{20} of the FCA-PEG surfactants indicate that their molecules prefer to form micelles rather than adsorb at the water/air interface.[30,37]

3.5 Flocculating properties of the FCA-PEG surfactants

Thanks to the unique combination of surface-active and high-molecular-weight properties, flocculants play an important role in the treatment of industrial and natural waste water.[53,54,55,56] They significantly accelerate the formation and aggregation of flocs from highly dispersed impurity particles, thereby facilitating their removal from water via sedimentation or filtration. For this reason, flocculants are widely used in various industrial processes, including the mining, oil and gas, pulp and paper industries. However, despite the diversity of existing flocculants, their application does not always yield the desired results. The primary reason for this may be the high cost or complex synthesis of the starting compounds required for flocculant production. Another reason may be the insufficient efficiency of precipitating specific dispersed particles in suspension through flocculant action. Therefore, the development of new effective flocculants based on affordable and renewable plant-derived raw materials, and the expansion of their range, is an important and urgent task.

We investigated the flocculating properties of the synthesized nonionic surfactants based on FCA-PEG. The results are presented in Fig. 6 – 8. As shown in the figures, bentonite clay particles settle very slowly on their own, and only after two hours does the degree of suspension clarification (i.e., particle sedimentation) reach approximately 55% (curve 1, Fig. 6).

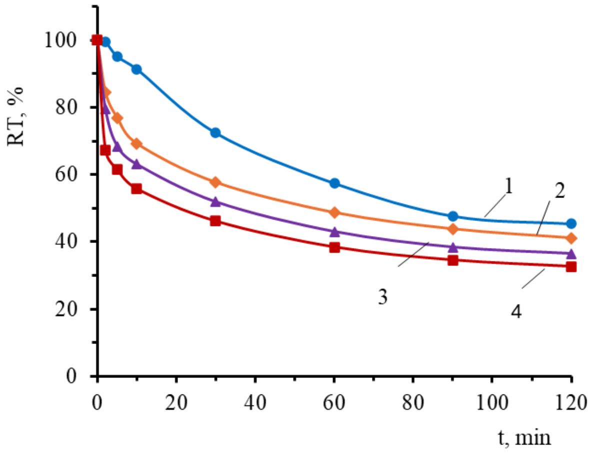

Flocculant dosage, mg/g clay: 0 (1); 0.1 (2); 0.2 (3); and 0.4 (4). Suspension concentration = 0.3 wt. %.

Fig. 6: Effect of FCA-PEG-300 surfactant on the flocculation rate of bentonite suspension particles.

In contrast, in the presence of FCA-PEG surfactants, the sedimentation process occurs significantly faster. The sedimentation rate depends on the molecular weight of PEG, and as the molecular weight of polyethylene glycol in FCA-PEG increases, the flocculating ability of the compound improves. The most pronounced acceleration of particle settling is observed in the presence of FCA-PEG-600. For example, in this case, after 30 minutes the suspension clarification reaches approximately 96% (Fig. 7).

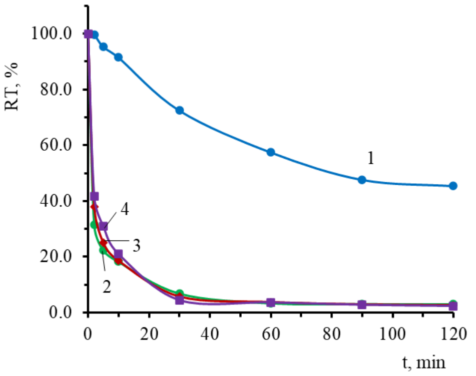

Flocculant dosage, mg/g clay: 0 (1); 0.1 (2); 0.2 (3); and 0.4 (4). Suspension concentration = 0.3 wt.%.

Fig. 7: Effect of FCA-PEG-600 surfactant on the flocculation rate of bentonite suspension particles.

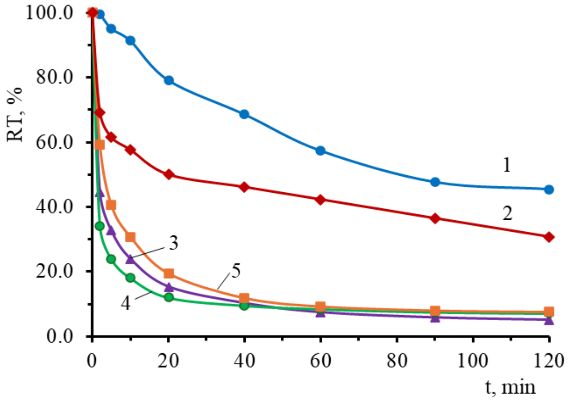

Flocculant dosage, mg/g clay: 0 (1); 0.1 (2); 0.1 (3); 0.2 (4); and 0.4 (5). Suspension concentration = 0.3 wt. %.

Fig. 8: Effect of PEG-1000 (2) and FCA-PEG-1000 surfactant (3–5) on the flocculation rate of bentonite suspension particles.

According to the elemental analysis by X-ray fluorescence spectroscopy, bentonite clay consists predominantly (over 99%) of silicon dioxide (73.3%), aluminum oxide (18.0%), iron (III) oxide (6.20%), calcium oxide (0.88%), and titanium dioxide (0.72%) (Table 5).

Consequently, it can be assumed that bentonite clay is essentially a mixture of silicic acid salts (metal silicates), and due to the dissociation of metal silicates in suspension, a negative charge forms on the surface of the dispersed particles.

Table 5: Results of the elemental composition analysis of bentonite clay FP by X-ray fluorescence spectroscopy. Analyzed Result (FP method).

No	Component	Content, mass %	No	Component	Content, mass %
1.	MgO	No Date	9.	Fe_2O_3	6.20
2.	Al_2O_3	18.0	10.	Br	0.0006
3.	SiO_2	73.3	11.	I	No Date
4.	P_2O_5	0.022	12.	Na_2O	No Date
5.	Cl	0.492	13.	Sc	No Date
6.	K_2O	0.0271	14.	Y	0.0015
7.	CaO	0.879	15.	V	0.0119
8.	TiO_2	0.716	16.	Cr	0.0064

To clarify the mechanism of particle flocculation, the change in the zeta potential of bentonite clay particles in the presence of FCA-PEG-1000 surfactant was measured (Fig. 9).

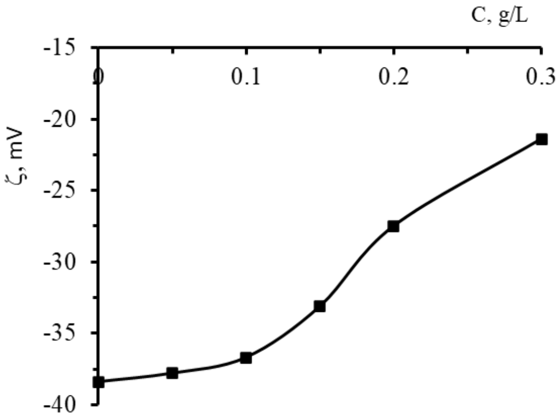

Fig. 9: Effect of FCA-PEG-1000 surfactant concentration on the zeta potential of bentonite suspension particles.

As seen in the figure, the suspension particles carry a negative charge and exhibit a zeta potential of –38 mV. In,[57] it was found that the zeta potential of bentonite clay particles depends not only on the pH of the medium, but also on the electrolyte concentration. For example, in demineralized water, when the pH changes from 2 to 11, the zeta potential of the particles decreases from –21 mV to –33 mV. In contrast, in tap water, the same change in acidity leads to a decrease in zeta potential from –13 mV to –18 mV.

In,[44] the zeta potential of bentonite clay suspension particles was –25 mV. Minor differences in the zeta potential of bentonite clays from different deposits are most likely due to the variations in clay composition.

As seen from Fig. 9, the presence and increasing concentration of FCA-PEG-1000 surfactant lead to a monotonic decrease in the negative charge (zeta potential) of the suspension particles. At a surfactant concentration of 0.3 g/L, the zeta potential decreases by 17 mV and reaches –21 mV.

Taking into account the chemical composition of bentonite clay, the following explanation can be proposed. The main component of bentonite clay (more than 73.3%) is silicon dioxide. According to Table 4, the molar ratio of silicon dioxide to metal oxides is approximately 1:0.4. That is, the molar amount of silicon dioxide in the clay is 2.5 times higher than that of metal oxides. Therefore, it can be assumed that about 40–50 mol. % of silicon dioxide reacts with metal oxides and forms metal silicates, while the remaining portion (~50 mol. %) is present in a free state.

In an aqueous medium, silicon dioxide absorbs water and transforms into silicic acid Eq. (9):

$$SiO_2 + H_2O = H_2SiO_3 \tag{9}$$

Silicic acid, being a dibasic weak acid (dissociation constants $K_1 = 2\times10^{-10}$, $K_2 = 2\times10^{-12}$), dissociates into ions, resulting in the formation of hydrogen cations and a silicate anion Eq. (10):[58]

$$H_2SiO_3 = 2H^+ + SiO_3^{2-} \tag{10}$$

As a result, the surface of bentonite clay particles acquires a negative charge. Apparently, in the presence of FCA-PEG surfactants in the suspension, the dissociation of silicic acid molecules is suppressed, and the chemical equilibrium (10) shifts toward the formation of molecular acid. Consequently, the surface charge (zeta potential) of the particles decreases, and upon reaching a “critical” zeta potential value, the suspension particles lose stability, leading to coagulation.[44]

At the same time, the possibility that PEG macromolecules interact with silicic acid through hydrogen bonding cannot be ruled out.[50,59,60] In this case, FCA-PEG surfactant macromolecules may simultaneously interact with the surface of several suspension particles via a bridging mechanism. As a result, the hydrophobicity of FCA-PEG macromolecules increases (their solubility decreases), and they undergo coiling (compaction). This leads to the agglomeration of several clay suspension particles into one larger particle, which then settles to the bottom due to gravity.

According to,[61] there are three distinct mechanisms of particle flocculation in suspensions:

1. *Coagulation:* in this case, a polyelectrolyte reduces or neutralizes the charge of suspension particles, resulting in particle aggregation.
2. *Electrostatic patch flocculation:* in this mechanism, adsorption of polymer macromolecules on localized regions of the particle surface leads to a local charge reversal, which promotes electrostatic attraction between positively and negatively charged sites of different particles.
3. *Polymer bridging:* in this process, segments of a polymer chain are simultaneously adsorbed onto the surfaces of multiple particles. As a result, particles aggregate into a larger entity and settle under the influence of gravity.

Thus, considering the above and the obtained experimental data, it can be concluded that the flocculation of bentonite clay particles in the presence of FCA-PEG surfactants occurs due to the reduction in particle surface charge and the adsorption of flocculant macromolecules onto particle surfaces via a bridging mechanism. When the charge (zeta potential) decreases to a “critical” value, the attractive forces between particles outweigh the repulsive ones, leading to particle aggregation (coagulation).

According to the second mechanism, segments of the FCA-PEG macromolecule simultaneously adsorb onto the surfaces of multiple suspension particles through hydrogen bonding.[50,59,60] As a result, several suspension particles aggregate into a single larger one and settle to the bottom under the influence of gravity.[62,63] Ultimately, this leads to the removal of dispersed bentonite clay particles from wastewater.

Thus, among FCA-PEG surfactants, FCA-PEG-600 has the best flocculant effect, and its optimal dosage for flocculation of suspension particles is 0.2 mg/g (200 g/t of dry solids).

In[64] the effect of the polyacrylamide-based industrial anionic flocculant (Zetag 4110) with the apparent viscosity 1700 mPas at 1% concentration (10 g/L) on the flocculation of clay particles was studied. It was observed that the optimum flocculant dosage depends on the amound of cations present in the system. Therefore for clay suspensions prepared in demineralized water, the optimal flocculant dose (<1 mg/g) is less than for suspensions prepared in tap water (2.3 mg/g).

The optimal dose of Praestol flocculant depends on the type of flocculant, its application and the characteristics of the processed material (*e.g* type of sludge, its dry solid, suspension). For mechanical dewatering of sludge, doses can range from 80-300 g to 2-8 kg per ton of dry solids.

Thus, the optimal dose (0.2 mg/g) of the flocculant FCA-PEG-600 is lower than that of the flocculants Zetag and Praestol. This indicates an efficiency and cost-effectiveness of the use of the flocculant FCA-PEG-600. Another advantage of the FSA-PEG flocculant is that it is biodegradable.

4. Conclusion

Gas chromatography–mass spectrometry (GC–MS) analysis revealed that the mixture of fatty carboxylic acids (FCA) obtained from technical-grade vegetable oil consists of nine types of saturated and unsaturated carboxylic acids. The major components were identified as 9,12-octadecadienoic acid (linoleic acid) and 9-octadecenoic acid (oleic acid).

Nonionic surfactants were synthesized via the esterification of the FCA mixture with polyethylene glycol (PEG) of molecular weights 300, 600, and 1000 in the presence of p-toluenesulfonic acid as a catalyst. The reaction yield, calculated based on the acid number of the mixture, was 93–94%. The formation of FCA-PEG esters was confirmed by IR and NMR spectroscopy.

From the surface tension isotherms of aqueous solutions of the synthesized FCA-PEG surfactants, the critical micelle concentration, Gibbs adsorption at the water/air interface, surface area per molecule in the saturated adsorption layer, and other adsorption parameters were determined. Among the synthesized surfactants, FCA-PEG-600 exhibited the highest surface activity (Π_{CMC} = 28.8 mN/m). This anomalous behavior is attributed to the optimal hydrophilic–lipophilic balance of the FCA-PEG-600 macromolecule.

Among the synthesized surfactants, FCA-PEG-600 also showed the highest adsorption ($\Gamma_{max} = 3.0\times10^{-6}$ mol/m^2) and the smallest surface area (A_{min} = 0.55 nm^2) occupied by a single molecule in the saturated adsorption layer. These findings indicate that FCA-PEG-600 molecules adopt a more compact conformation, stabilized by hydrophobic interactions between hydrocarbon chains and hydrogen bonding between hydroxyl groups, in comparison to other FCA-PEG surfactants.

Investigation of the flocculation behavior of bentonite clay suspensions in the presence of the surfactants demonstrated that FCA-PEG compounds exhibit flocculating activity. FCA-PEG-600 exhibited the highest flocculation performance among the synthesized surfactants. Its optimal dosage for flocculation of suspension's particles was 0.2 mg/g (200 g/t of dry solids).

Zeta potential measurements revealed that flocculation of bentonite clay particles in the presence of FCA-PEG surfactants occurs due to a reduction in the surface charge of the particles and the adsorption of the flocculant macromolecules via a bridging mechanism. Collectively, these effects lead to the destabilization of the suspension's particles.

Acknowledgments

This research has been funded by the Science Committee of the Ministry of Science and High Education of the Republic of Kazakhstan (Grant No. AP19678114).

Conflict of Interest

There are no conflict to declare.

Supporting Information

Applicable.

CRediT Statement

K. Zh. Abdiyev and **B. B. Sadykov:** Conceptualization; **M. B. Zhursumbayeva:** Methodology, **G. K. Kussainova** and **Zh. Toktarbay:** Software, **M. B. Zhursumbayeva, N. Zh. Seitkaliyeva** and **Z. N. Kambarova:** Validation, **Zh. Toktarbay:** Formal analysis, **G. K. Kussainova, M. B. Zhursumbayeva, N. Zh. Seitkaliyeva** and **Z. N. Kambarova:** Investigation, **Z. N. Kambarova:** Resources, **Zh. Toktarbay** and **M. B. Zhursumbayeva:** Data curation, **K. Zh. Abdiyev** and **B. B. Sadykov:** Writing - Original draft preparation, **K. Zh. Abdiyev** and **Chien-Hsiang Chang:** Writing - Review and editing, **Zh. Toktarbay** and **Chien-Hsiang Chang:** Visualization, **K. Zh. Abdiyev** and **B. B. Sadykov:** Supervision, **K. Zh. Abdiyev:** Funding acquisition, **K. Zh. Abdiyev:** Project administration. All authors have read and agreed to the published version of the manuscript.

References

[1] N. Baccile, Bio-based surfactants and green soft materials, *Encyclopedia of Green Chemistry*, 2025, **1**, 389-402, doi: 10.1016/b978-0-443-15742-4.00044-2.

[2] O. J. Fisher, J. Sadhukhan, T. Daniel, J. Xuan, Techno-economic analysis and process simulation of alkoxylated surfactant production in a circular carbon economy framework, *Digital Chemical Engineering*, 2024, **13**, 100199, doi: 10.1016/j.dche.2024.100199.

[3] M. Kjellin, I. Johansson, Surfactants from Renewable Resources, *wiley Online Library*, 2010, doi: 10.1002/9780470686607.

[4] T. Benvegnu, D. Plusquellec, L. Lemiègre, Surfactants from renewable sources: synthesis and applications, *Monomers, Polymers and Composites from Renewable Resources*, 2008, 153-178, doi: 10.1016/b978-0-08-045316-3.00007-7.

[5] P. S. Piispanen, M. Persson, P. Claesson, T. Norin, Surface

properties of surfactants derived from natural products. Part 1: Syntheses and structure/property relationships: Solubility and emulsification, *Journal of Surfactants and Detergents*, 2004, **7**, 147-159, doi: 10.1007/s11743-004-0298-6.

[6] K. Toshtay, Liquid-phase hydrogenation of sunflower oil over platinum and nickel catalysts: Effects on activity and stereoselectivity, *Results in Engineering*, 2024, **21**, 101970, doi: 10.1016/j.rineng.2024.101970.

[7] N.-S. Mussa, K. Toshtay, M. Capron, Catalytic applications in the production of hydrotreated vegetable oil (HVO) as a renewable fuel: a review, *Catalysts*, 2024, **14**(7), 452, doi: 10.3390/catal14070452.

[8] H. Lu, G. Pourceau, B. Briou, A. Wadouachi, T. Gaudin, I. Pezron, A. Drelich, Sugar-based surfactants: effects of structural features on the physicochemical properties of sugar esters and their comparison to commercial octyl glycosides, *Molecules*, 2024, **29**(10), 2338, doi: 10.3390/molecules29102338.

[9] W. Xiang, B. Tardy, L. Bai, C. Stubenrauch, O. J. Rojas, Measuring the interfacial behavior of sugar-based surfactants to link molecular structure and uses, *Biobased Surfactants*, 2019, 387-412, doi: 10.1016/b978-0-12-812705-6.00012-5.

[10] W. Ruback, S. Schmidt, Alkyl polyglucoside, a carbohydrate-based surfactant, *Carohydrates as Organic Raw Materials III*, 1996, doi: 10.1002/9783527614899.ch13.

[11] E. Jurado, V. Bravo, G. Luzón, M. Fernández-Serrano, M. García-Román, D. Altmajer-Vaz, J. M. Vicaria, Hard-surface cleaning using lipases: enzyme–surfactant interactions and washing tests, *Journal of Surfactants and Detergents*, 2007, **10**, 61-70, doi: 10.1007/s11743-006-1009-z.

[12] E. Jurado, J. M. Vicaria, A. Fernandez-Arteaga, P. Chachalis, J. F. García-Martín, Wetting power in aqueous mixtures of alkylpolyglucosides and ethoxylated fatty alcohols, *Journal of Surfactants and Detergents*, 2010, **13**, 497-501, doi: 10.1007/s11743-010-1228-1.

[13] M. Lukosek, M. Emmons-Burzyńska, K. Alejski, I. Szwach, Physicochemical characterization of ethoxylation products of fatty acid esters, *Frontiers in Chemical Engineering*, 2021, **3**, 617701, doi: 10.3389/fceng.2021.617701.

[14] D. G. Hayes, Fatty acids–based surfactants and their uses, *Fatty Acids*, 2017, 355-384, doi: 10.1016/b978-0-12-809521-8.00013-1.

[15] I. Johansson, M. Svensson, Surfactants based on fatty acids and other natural hydrophobes, *Current Opinion in Colloid & Interface Science*, 2001, **6**, 178-188, doi: 10.1016/s1359-0294(01)00076-0.

[16] M. R. Behera, S. R. Varade, P. Ghosh, P. Paul, A. S. Negi, Foaming in Micellar Solutions: Effects of Surfactant, Salt, and Oil Concentrations, *Industrial & Engineering Chemistry Research*, 2014, **53**, 18497–18507, doi: 10.1021/ie503591v.

[17] A. K. N. University, S. Turganbay, S. B. Aidarova, G. Turganbay, Y. Tileuberdi, S.-L. Chen, Synthesis and characterization of sulfur nanoparticles with WSP/surfactants mixtures, *International Journal of Biology and Chemistry*, 2019, **12**, 146-152, doi: 10.26577/ijbch-2019-1-i19.

[18] R. Li, Y. Lu, Z. Zhang, R. Manica, Role of surfactants based on fatty acids in the wetting behavior of solid–oil–aqueous solution systems, *Langmuir*, 2021, **37**(18), 5682-5690, doi: 10.1021/acs.langmuir.1c00586.

[19] J. H. Lee, S. W. Jung, I. S. Kim, Y. I. Jeong, Y. H. Kim, S. H. Kim, Polymeric nanoparticle composed of fatty acids and poly (ethylene glycol) as a drug carrier, *International journal of pharmaceutics*, 2003, **251**, 23-32, doi: 10.1016/S0378-5173(02)00582-3.

[20] G. Gaucher, M.-H. Dufresne, V. P. Sant, N. Kang, D. Maysinger, J.-C. Leroux, Block copolymer micelles: preparation, characterization and application in drug delivery, *Journal of Controlled Release*, 2005, **109**, 169-188, doi: 10.1016/j.jconrel.2005.09.034.

[21] S. Biswas, N. S. Dodwadkar, R. R. Sawant, V. P. Torchilin, Development of the novel PEG-PE-based polymer for the reversible attachment of specific ligands to liposomes: synthesis and *in vitro* characterization, *Bioconjugate Chemistry*, 2011, **22**, 2005-2013, doi: 10.1021/bc2002133.

[22] A. Rösler, G. W. M. Vandermeulen, H.-A. Klok, Advanced drug delivery devices *via* self-assembly of amphiphilic block copolymers, *Advanced Drug Delivery Reviews*, 2012, **64**, 270-279, doi: 10.1016/j.addr.2012.09.026.

[23] M. S. Bakshi, Colloidal micelles of block copolymers as nanoreactors, templates for gold nanoparticles, and vehicles for biomedical applications, *Advances in Colloid and Interface Science*, 2014, **213**, 1-20, doi: 10.1016/j.cis.2014.08.001.

[24] Y. Lu, L. Huang, W. Chen, Probing the role of hydrophobic groups on the performance of fatty acid surfactants for hematite flotation, *Journal of Molecular Liquids*, 2024, **411**, 125674, doi: 10.1016/j.molliq.2024.125674.

[25] Z. Wang, Q. Lu, J. Wang, J. Liu, G. Liu, W. Sun, L. Xie, Q. Liu, H. Zeng, Nanomechanical insights into hydrophobic interactions of mineral surfaces in interfacial adsorption, aggregation and flotation processes, *Chemical Engineering Journal*, 2023, **455**, 140642, doi: 10.1016/j.cej.2022.140642.

[26] M. Almeida, B. Couturaud, B. Rousseau, D. Dudzinski, S. Prévost, C. Amiel, F. Cousin, C. Le Coeur, Pegylated surfactants based on fatty acids: 12-hydroxystearic acid versus stearic acid, *Journal of Molecular Liquids*, 2024, **411**, 125723, doi: 10.1016/j.molliq.2024.125723.

[27] J.-J. Liu, M. A. A. Gasmalla, P. Li, R. Yang, Enzyme-assisted extraction processing from oilseeds: Principle, processing and application, *Innovative Food Science & Emerging Technologies*, 2016, **35**, 184-193, doi: 10.1016/j.ifset.2016.05.002.

[28] X. Liu, Y. Zhao, Q. Li, J. Niu, Surface tension, interfacial tension and emulsification of sodium dodecyl sulfate extended surfactant, *Colloids and Surfaces A: Physicochemical and Engineering Aspects*, 2016, **494**, 201-208, doi: 10.1016/j.colsurfa.2016.01.037.

[29] M. Lv, Y. Zhou, S. Wang, F. Han, B. Xu, Effects of the polypropylene oxide number on the surface properties of a type of extended surfactant, *Journal of Surfactants and Detergents*, 2018, **21**, 335-341, doi: 10.1002/jsde.12039.

[30] Y. Gagnon, H. Mhemdi, F. Delbecq, E. Van Hecke, Extended surfactants and their tailored applications for vegetable oils

extraction: an overview, *Oilseeds & fats crops and Lipids*, 2021, **28**, 7, doi: 10.1051/ocl/2020062.

[31] A. M. Forgiarini, C. Scorzza, J. Velásquez, F. Vejar, E. Zambrano, J.-L. Salager, Influence of the mixed propoxy/ethoxy spacer arrangement order and of the ionic head group nature on the adsorption and aggregation of extended surfactants, *Journal of Surfactants and Detergents*, 2010, **13**, 451-458, doi: 10.1007/s11743-010-1216-5.

[32] K. Z. Abdiyev, B. B. Sadykov, M. B. Zhursumbayeva, N. Z. Seitkaliyeva, C.-H. Chang, G. K. Kussainova, Z. N. Kambarova, Z. Toktarbay, New nonionic surfactants from renewable raw materials-sunflower oil production waste, *ES Materials & Manufacturing*, 2025, **29**, 1679, doi: 10.30919/mm1679.

[33] A. V. Falaleev,_I. V. Voronyuk, A. A. Kruzhilin, Kh. Shikhaliev, GC-MS analysis of N,N-dimethylaminopropylamides of fatty acids of vegetable oils, *Sorption & Chromatogr Processes*, 2014, **14**(3), 494-501.

[34] K. Toshtay, A. Auyezov, Z. Korkembay, S. Toktassynov, A. Seytkhan, A. Nurakyshev, Partial hydrogenation of sunflower oil on platinum catalysts: Influence of process conditions on the mass content of geometric isomers, *Molecular Catalysis*, 2021, 513, 111819, doi: 10.1016/j.mcat.2021.111819.

[35] A. Atrafi, M. Pawlik, Surface tension and gas dispersion properties of fatty acid solutions, *Minerals Engineering*, 2016, **85**, 138-147, doi: 10.1016/j.mineng.2015.11.006.

[36] J. T. Davies, E. K. Rideal, Interfacial phenomena. New York-London: Academic Press, 1963, 2, *Angewandte Chemie*, 1965, **77**(6), 276, doi: 10.1002/ange.19650770625.

[37] P. Szumała, A. Mówińska, Perfectly wetting mixtures of surfactants from renewable resources: the interaction and synergistic effects on adsorption and micellization, *Journal of Surfactants and Detergents*, 2016, **19**, 437-445, doi: 10.1007/s11743-016-1793-z.

[38] D. K. Chattoraj, K. S. Birdi, Adsorption and the Gibbs Surface Excess, 1984, New York, doi: 10.1007/978-1-4615-8333-2.

[39] J. T. Davies, The distribution of ions under a charged monolayer, and a surface equation of state for charged films, *Proceedings of the Royal Society of London Series A Mathematical and Physical Sciences*, 1951, **208**, 224-247, doi: 10.1098/rspa.1951.0156.

[40] K. S. Birdi, *Surface and Colloid Chemistry. Principles and Applications*, Boca Raton, 2009, 228, doi: 10.1201/b10154.

[41] M. J. Rosen, D. S. Murphy, Effect of the nonaqueous phase on interfacial properties of surfactants. 2. Individual and mixed nonionic surfactants in hydrocarbon/water systems, *Langmuir*, 1991, **7**, 2630-2635, doi: 10.1021/la00059a039.

[42] O. Y. Berezin, Y. I. Tur'yan, L. Kogan, I. Kuselman, A. Shenhar, Practical limitations in determining vegetable oil acid values by a novel pH-metric method, *Journal of the American Oil Chemists' Society*, 1997, **74**, 1339-1341, doi: 10.1007/s11746-997-0067-3.

[43] B. Zhang, H. Su, X. Gu, X. Huang, H. Wang, Effect of structure and charge of polysaccharide flocculants on their flocculation performance for bentonite suspensions, *Colloids and Surfaces A: Physicochemical and Engineering Aspects*, 2013, **436**, 443-449, doi: 10.1016/j.colsurfa.2013.07.017.

[44] K. Z. Abdiyev, Z. Toktarbay, A. Z. Zhenissova, M. B. Zhursumbaeva, R. N. Kainazarova, N. Nuraje, The new effective flocculants–Copolymers of N, N-dimethyl-N, N-diallyl-ammonium chloride and N, N-dimethylacrylamide, *Colloids and Surfaces A: Physicochemical and Engineering Aspects*, 2015, **480**, 228-235, doi: 10.1016/j.colsurfa.2015.04.025.

[45] A. Ardakkyzy, A. Zulkarnayev, A. Sarsengaliyeva, N. Abeu, Y. Tileuberdi, Z. Toktarbay, N. Nuraje, Tunable oil-water separation using engineered cellulose membranes, *Chemosphere*, 2025, **382**, 144319, doi: 10.1016/j.chemosphere.2025.144319.

[46] I. Fleming, & D. H. Williams, *Spectroscopic methods in organic chemistry*, Springer Cham, 1996, doi: 10.1007/978-3-030-18252-6.

[47] G. A. Smith, Fatty acid, methyl ester, and vegetable oil ethoxylates, *Biobased Surfactants*, 2019, 287-301, doi: 10.1016/b978-0-12-812705-6.00008-3.

[48] K. S. Birdi, *Surface and colloid chemistry:principles and applications*, 2009, **13**, 978-1-4200-9504-3.

[49] E. M. Shaikhutdinov, S. K. Khussain, K. Z. Abdiyev, N. Z. Seitkaliyeva, Complexation of sodium 2-acrylamido-2-methylpropanesulfonate-monoethanolamine vinyl ether copolymer with polyelectrolytes in aqueous medium, *Polymer Science Series A*, 2007, **49**, 584-592, doi: 10.1134/s0965545x07050136.

[50] K. Z. Abdiyev, E. M. Shaikhutdinov, M. B. Zhursumbaeva, S. K. Khussain, Effect of polymer concentration on the surface properties of polyacid–poly(N-vinylpyrrolidone) complexes, *Colloid Journal*, 2003, **65**, 399-402, doi: 10.1023/A:1025105631381.

[52] A. A. Trapeznikov, V. G. Vins, T. Yu. Shirokova, Kinetics of surface tension reduction in protein solutions, *Colloid Journal*, 1981, **43**(2), 322-329.

[53] Y. Sun, Sh. Zhou, K. J. Shah, New Class of Flocculants and Coagulants, *Materials Research Foundations*, 2021, **91**, 219-252, doi: 10.21741/9781644901144-7.

[54] J. Jumadi, A. Kamari, J. S. J. Hargreaves, N. Yusof, A review of nano-based materials used as flocculants for water treatment, *International Journal of Environmental Science and Technology*, 2020, **17**, 3571-3594, doi: 10.1007/s13762-020-02733-y.

[55]. A. K. Badawi, R. S. Salama, M. M. M. Mostafa, Natural-based coagulants/ flocculants as sustainable market-valued products for industrial wastewater treatment: a review of recent developments, *RSC Advances*, 2023, **13**, 19335-19355.

[56] K. Z. Abdiyev, M. Maric, B. Y. Orynbayev, Z. Toktarbay, M. B. Zhursumbaeva, N. Z. Seitkaliyeva, Flocculating properties of 2-ac rylamido-2-methyl-1-propanesulfonic acid-co-allylamine polyampholytic copolymers, *Polymer Bulletin*, 2022, **79**, 10741-10756, doi: 10.1007/s00289-021-03994-2.

[57] J. Li, X. Song, J. Pan, L. Zhong, S. Jiao, Q. Ma, Adsorption and flocculation of bentonite by chitosan with varying degree of deacetylation and molecular weight, *International Journal of Biological Macromolecules*, 2013, **62**, 4-12, doi: 10.1016/j.ijbiomac.2013.08.009.

[58] V. Lenher, Silicic acid, *Journal of the American Chemical Society*, 1921, **43**, 391-396, doi: 10.1021/ja01436a002.

[59] S. V. Patwardhan, C. Raab, N. Hüsing, S. J. Clarson, Macromolecule mediated bioinspired silica synthesis using a diol-modified silane precursor, *Silicon Chemistry*, 2005, **2**, 279-285, doi: 10.1007/s11201-005-3416-9.

[60] C. Alkan, E. Günther, S. Hiebler, M. Himpel, Complexing blends of polyacrylic acid-polyethylene glycol and poly(ethylene-co-acrylic acid)-polyethylene glycol as shape stabilized phase change materials, *Energy Conversion and Management*, 2012, **64**, 364-370, doi: 10.1016/j.enconman.2012.06.003.

[61] J. Gregory, Rates of flocculation of latex particles by cationic polymers, *Journal of Colloid and Interface Science*, 1973, **42**, 448-456, doi: 10.1016/0021-9797(73)90311-1.

[62] L. Besra, D. K. Sengupta, S. K. Roy, P. Ay, Polymer adsorption: its correlation with flocculation and dewatering of Kaolin suspension in the presence and absence of surfactants, *International Journal of Mineral Processing*, 2002, **66**, 183-202, doi: 10.1016/s0301-7516(02)00064-9.

[63] Y. Yeszhan, K. Bexeitova, S. Yermekbayev, Z. Toktarbay, J. Lee, R. Berndtsson, S. Azat, Photocatalytic degradation of microplastics in aquatic environments: materials, mechanisms, practical challenges, and future perspectives, *Water*, 2025, **17**, 2139, doi: 10.3390/w17142139.

[64] A. Shakeel, Z. Safar, M. Ibanez, L. van Paassen, C. Chassagne, Flocculation of clay suspensions by anionic and cationic polyelectrolytes: a systematic analysis, *Minerals*, 2020, **10**(11), 999, doi: 10.3390/min10110999.

Open Access